Contribution from the Chemistry Department, 227-PSB UAB Station, The University of Alabama at Birmingham, Birmingham, Alabama 35294

Syntheses and Reactions of the *cis*-$PtCl_2\{Ph_2P(CH_2CH_2O)_nCH_2CH_2PPh_2\text{-}P,P'\}$ (n = 3-5) Metallacrown Ether Complexes. The X-ray Crystal Structures of the n = 4 and 5 Complexes and of [*cis*-$Pt\{Ph_2P(CH_2CH_2O)_4CH_2CH_2PPh_2\text{-}P,P',O\}(H_2O)](BF_4)_2$

Ashima Varshney, Mary L. Webster, and Gary M. Gray*

Received October 23, 1991

Metallacrown ether complexes of the type $PtCl_2\{Ph_2P(CH_2CH_2O)_nCH_2CH_2PPh_2\}$ (n = 3-5) have been prepared and characterized by ^{13}C and ^{31}P NMR spectroscopy. A single complex is formed with the n = 3 and 4 ligands, and one major and two minor complexes are formed with the n = 5 ligand. X-ray crystal structures of the n = 4 and major n = 5 complexes have been obtained (n = 4: monoclinic space group $P2_1/n$; a = 12.798 (1), b = 16.4875 (9), c = 16.726 (1) Å; β = 104.003 (6)°; V = 3424.4 Å^3; Z = 4. n = 5: monoclinic space group $P2_1/c$; a = 12.9220 (9), b = 15.5925 (8), c = 18.3271 (5) Å; β = 92.540 (5)°, V = 3689.0 Å^3; Z = 4). The metallacrown ether rings in both complexes exhibit similar conformations. The cavity in the n = 4 complex appears to be of the appropriate size for binding Li^+ and that in the n = 5 complex appears to be of the appropriate size for binding Na^+. The complexes do appear to coordinate alkali metal cations, but these reactions are complicated by solubility differences and by loss of the chlorides. The n = 4 complex reacts with $AgBF_4$ to yield the cationic $[Pt\{Ph_2P(CH_2CH_2O)_4CH_2CH_2PPh_2\text{-}P,P',O\}(H_2O)](BF_4)_2$ complex. The X-ray crystal structure of this complex has been determined (triclinic space group $P\bar{1}$; a = 9.971 (2), b = 10.293 (2), c = 20.212 (5) Å; α = 80.92 (2), β = 84.92 (2), γ = 75.48 (1)°; V = 1980.3 Å^3; Z = 2). The $Ph_2P(CH_2CH_2O)_4CH_2CH_2PPh_2$ ligand is coordinated to the platinum through both phosphines and one ether oxygen and is also hydrogen bonded to the platinum-coordinated water through two other ether oxygens.

Introduction

A number of transition metal complexes of α,ω-bis(phosphine)-polyether ligands,[1-8] α,ω-bis(phosphinite)- or α,ω-bis(phosphite)-polyether ligands,[9-15] and cyclic diphosphacrown ether ligands[16,17] (metallacrown ethers) have been reported. The metallacrown ether rings in these complexes provide coordination sites for hard metal ions and exhibit size selectivities toward alkali metal cations. These properties may allow these complexes to exhibit unusual catalytic activities and selectivities, to serve as phase-transfer catalysts, and/or to activate small molecules. This latter application is of particular interest because it may allow these complexes to activate ligands such as CO and CO_2 via coordination of the carbon atom to the transition metal and the oxygen atom to the alkali metal cation and ligands such as hydroxide, water, ammonia, and hydroxycarbonyl by coordination to the transition metal and hydrogen bonding to the ethers.

The most versatile ligands employed in these complexes are the α,ω-bis(phosphine)-polyether ligands. In contrast to the α,ω-bis(phosphinite)- and α,ω-bis(phosphite)-polyether ligands, they cannot undergo Arbuzov dealkylations[18-20] and thus should form stable complexes with platinum-group metals. In contrast to the diphosphacrown ether ligands, they are much easier to synthesize but still form mononuclear transition metal complexes. As we have recently reported, metallacrown ethers of these ligands of the type *cis*-$Mo(CO)_4\{Ph_2P(CH_2CH_2O)_nCH_2CH_2PPh_2\}$ (n = 4, 5) form isolable complexes with alkali metal cations.[8] The ring size in these complexes determines the alkali metal cation selectivity, with the n = 4 complex binding most strongly to Li^+ and the n = 5 complex binding most strongly to Na^+.

The molybdenum carbonyl complexes are not suitable for the applications described above. We have now extended our work to include metallacrown ether complexes containing platinum-group metals that may be suitable for these applications. In this paper, we report the syntheses and spectroscopic characterizations of a variety of platinum(II) metallacrown ether complexes. The implications of the NMR spectroscopic data as to the solution conformations of the complexes are discussed, and the interactions of the complexes with alkali metal salts are described. X-ray crystal structures of three of the complexes, *cis*-$PtCl_2\{Ph_2P(CH_2CH_2O)_nCH_2CH_2PPh_2\}$ (n = 4, 5) and $[Pt\{Ph_2P(CH_2CH_2O)_4CH_2CH_2PPh_2\text{-}P,P',O\}(H_2O)](BF_4)_2$, have been determined, and these are presented.

Experimental Section

The $^{31}P\{^1H\}$ and $^{13}C\{^1H\}$ NMR spectra were recorded on a GE NT-300, wide-bore, multinuclear NMR spectrometer. The ^{31}P NMR spectra are referenced to external 85% phosphoric acid, and the ^{13}C NMR spectra are referenced to internal tetramethylsilane. Chemical shifts downfield from those of the reference compounds are reported as positive. The ^{31}P and ^{13}C NMR data for the complexes are given in Tables I and II. Infrared spectra of KBr disks of the complexes were recorded on either a Nicolet IR44 spectrometer or a Perkin-Elmer 283B IR spectrometer. Elemental analyses were performed by Atlantic Microlab, Inc., Norcross, GA.

All free ligands, tetrahydrofuran (THF), and diethyl ether were handled under high-purity nitrogen, and all reactions and recrystallizations were carried out under high-purity nitrogen. The solid products were air stable. All solvents were of reagent grade and were used as received except for diethyl ether and THF, which were distilled from sodium-benzophenone. All starting materials were reagent grade and were used as received. The deuterated solvents were opened and handled under a nitrogen atmosphere at all times. The $Ph_2P(CH_2CH_2O)_nCH_2CH_2PPh_2$ (**1**, n = 3; **2**, n = 4; **3**, n = 5) ligands[8] and $PtCl_2(cod)$ (cod = 1,5-cyclooctadiene)[21,22] were prepared using standard procedures.

(1) Alcock, N. W.; Brown, J. M.; Jeffery, J. C. *J. Chem. Soc., Chem. Commun.* **1974**, 829.
(2) Alcock, N. W.; Brown, J. M.; Jeffery, J. C. *J. Chem. Soc., Dalton Trans.* **1976**, 583.
(3) Hill, W. E.; Taylor, J. G.; McAuliffe, C. A.; Muir, K. W.; Manojlovic-Muir, L. *J. Chem. Soc., Dalton Trans.* **1982**, 833.
(4) Thewissen, D. H. W.; Timmer, K.; Noltes, J. G.; Marsman, J. W.; Laine, R. M. *Inorg. Chim. Acta* **1985**, *97*, 143.
(5) Timmer, K.; Thewissen, D. H. W. *Inorg. Chim. Acta* **1985**, *100*, 235.
(6) Hill, W. E.; Taylor, J. G.; Falshaw, C. P.; King, T. J.; Beagley, B.; Tonge, D. M.; Pritchard, R. G.; McAuliffe, C. A. *J. Chem. Soc., Dalton Trans.* **1986**, 2289.
(7) Timmer, K.; Thewissen, D. H. W.; Marsman, J. W. *Recl. Trav. Chim. Pays-Bas* **1988**, *107*, 248.
(8) Varshney, A.; Gray, G. M. *Inorg. Chem.* **1991**, *30*, 1748.
(9) Powell, J.; Kuksis, A.; May, C. J.; Nyberg, S. C.; Smith, S. J. *J. Am. Chem. Soc.* **1981**, *103*, 5941.
(10) Powell, J.; Nyberg, S. C.; Smith, S. J. *Inorg. Chim. Acta* **1983**, *76*, L75.
(11) Powell, J.; Ng, K. S.; Ng, W. W.; Nyberg, S. C. *J. Organomet. Chem.* **1983**, *243*, C1.
(12) Powell, J.; Gregg, M.; Kuskis, A.; Meindl, P. *J. Am. Chem. Soc.* **1983**, *105*, 1064.
(13) Powell, J.; Gregg, M. R.; Kuksis, A.; May, C. J.; Smith, S. J. *Organometallics* **1989**, *8*, 2918.
(14) Powell, J.; Kuskis, A.; May, C. J.; Meindl, P. E.; Smith, S. J. *Organometallics* **1989**, *8*, 2933.
(15) Powell, J.; Gregg, M. R.; Meindl, P. E. *Organometallics* **1989**, *8*, 2942.
(16) Wei, L.; Bell, A.; Warner, S.; Williams, I. D.; Lippard, S. J. *J. Am. Chem. Soc.* **1986**, *108*, 8302.
(17) Wei, L.; Bell, A.; Ahn, K.-H.; Holl, M. M.; Warner, S.; Williams, I. D.; Lippard, S. J. *Inorg. Chem.* **1990**, *29*, 825.
(18) Kong, P.-C.; Roundhill, D. M. *Inorg. Chem.* **1972**, *11*, 749.
(19) Kong, P.-C.; Roundhill, D. M. *J. Chem. Soc., Dalton Trans.* **1974**, 187.
(20) Beaulieu, W. B.; Rauchfuss, T. B.; Roundhill, D. M. *Inorg. Chem.* **1975**, *14*, 1732.
(21) Chatt, J.; Vallarino, L. M.; Venanzi, L. M. *J. Chem. Soc.* **1957**, 3413.
(22) Whitesides, G. M. *J. Am. Chem. Soc.* **1978**, *98*, 6521.

0020-1669/92/1331-2580$03.00/0

Table I. ^{31}P and Phenyl ^{13}C NMR Data[a,b]

	P			ipso		ortho		meta		
compd	$\delta^{31}P$ (ppm)	$\lvert J(PtP)\rvert$ (Hz)	$\lvert ^2J(PP)\rvert$ (Hz)	$\delta^{13}C$ (ppm)	$\lvert J(PC)\rvert$ (Hz)	$\delta^{13}C$ (ppm)	$\lvert J(PC)\rvert$ (Hz)	$\delta^{13}C$ (ppm)	$\lvert J(PC)\rvert$ (Hz)	para $\delta^{13}C$ (ppm)
1[c]	−21.63 s			138.29 d	13[d]	132.66 d	19[e]	128.51 d	9[f]	128.36 s
2[c]	−21.68 s			138.17 d	12[d]	132.68 d	18[e]	128.56 d	12[f]	128.41 s
3[c]	−21.69 s			138.29 d	12[d]	132.71 d	17[e]	128.58 d	10[f]	128.41 s
4	5.69 sd	3622		131.57 aq	67[g]	133.39 aq	10[h]	128.06 aq	11[i]	130.73 s
5	5.19 sd	3635		*j*		133.20 aq	8[h]	128.19 aq	8[i]	130.69 s
6a	5.32 sd	3622		*j*		133.26 bs	11[h]	128.17 bs		130.71 s
6b	4.46 sd	3623		*j*		133.43 aq	9[h]	128.30 aq	10[i]	131.05 s
6c	−2.53 sd	3684								
7[k]	7.28 bsd	3630								
8	36.20 ddd	3684	15							
	4.59 ddd	4247	15							
9	6.40 bsd	2323		*j*		133.46 bs		128.58 bs		131.12 bs
10	22.71 bsd	4143								
	−1.50 bsd	4619								
11[k]	0.56 sd	3767		123.64 d	68[d]	134.38 d	9[e]	130.23 d	11[f]	134.00 s

[a] b, broad; s, singlet; d, doublet; sd, superimposed singlet and doublet; ddd, doublet and superimposed doublet of doublets; aq, apparent quintet. [b] Solvent, chloroform-d_1. [c] Data from ref 8. [d] $\lvert ^1J(PC)\rvert$. [e] $\lvert ^2J(PC)\rvert$. [f] $\lvert ^3J(PC)\rvert$. [g] $\lvert ^1J(PC) + {}^3J(PC)\rvert$. [h] $\lvert ^2J(PC) + {}^4J(PC)\rvert$. [i] $\lvert ^3J(PC) + {}^5J(PC)\rvert$. [j] Not observed. [k] Solvent, acetonitrile-d_3.

Table II. Aliphatic ^{13}C NMR Data[a]

	C1		C2		C3	C4	C5	C6
compd	$\delta^{31}C$ (ppm)	$\lvert J(PC)\rvert$ (Hz)	$\delta^{13}C$ (ppm)	$\lvert J(PC)\rvert$ (Hz)	$\delta^{13}C$ (ppm)	$\delta^{13}C$ (ppm)	$\delta^{13}C$ (ppm)	$\delta^{13}C$ (ppm)
1	28.77 d	13[b]	68.53 d	25[c]	70.10 s	70.57 s		
2	28.73 d	12[b]	68.53 d	26[c]	70.10 s	70.58 s	70.53 s	
3	28.73 d	13[b]	68.49 d	25[c]	70.07 s	70.55 s	70.51 s	70.51 s
4	27.87 aq	42[d]	68.59 bs		71.94 s	70.58 s		
5	27.79 aq	42[d]	67.73 bs		71.39 s	70.80 s	70.80 s	
6a	27.63 aq	37[d]	67.53 bs		70.97 s	70.70 s	70.62 s	70.62 s
6b	30.42 aq	41[d]	66.90 bs		69.87 s	70.33 s	70.47 s	70.47 s
9	29.74 bs				71.24 bs, 70.83 s, 70.21 s, 66.83 s			
11	28.16 d	42[b]			72.67 s, 71.28 s, 70.67 s, 62.27 s			

[a] b, broad; s, singlet; d, doublet; aq, apparent quintet. [b] $\lvert ^1J(PC)\rvert$. [c] $\lvert ^2J(PC)\rvert$. [d] $\lvert ^1J(PC) + {}^3J(PC)\rvert$. [e] $\lvert ^2J(PC) + {}^4J(PC)\rvert$.

***cis*-$PtCl_2\{Ph_2P(CH_2CH_2O)_3CH_2CH_2PPh_2\}$ (4).** A solution of 0.500 g (1.34 mmol) of $PtCl_2$(cod) in 50 mL of dichloromethane and a solution of 0.710 g (1.34 mmol) of **1** in 50 mL of dichloromethane were added simultaneously and dropwise to 50 mL of dichloromethane at ambient temperature over a 45-min period. This solution was stirred for 8 h and then evaporated to dryness to yield a white, powdery residue. This material was recrystallized from a dichloromethane–hexanes mixture to yield 0.94 g (88%) of analytically pure **4**·$0.5H_2O$ (mp 210–215 °C). Anal. Calcd for $C_{32}H_{37}Cl_2O_{3.5}P_2Pt$: C, 47.70; H, 4.60. Found: C, 47.53; H, 4.62. IR (KBr disk): ν(Pt–Cl) 307, 283 cm^{-1}.

***cis*-$PtCl_2\{Ph_2P(CH_2CH_2O)_4CH_2CH_2PPh_2\}$ (5).** By use of the procedure for **4**, 2.00 g (5.35 mmol) of $PtCl_2$(cod) and 3.07 g (5.35 mmol) of **2** yielded 4.70 g (100%) of **5**·$0.5H_2O$ (mp 215–220 °C) as a white powder. Anal. Calcd for $C_{34}H_{41}Cl_2O_{4.5}P_2Pt$: C, 48.06; H, 4.83. Found: C, 47.94; H, 4.85. IR (KBr disk): ν(Pt–Cl) 310, 284 cm^{-1}.

***cis*-$PtCl_2\{Ph_2P(CH_2CH_2O)_5CH_2CH_2PPh_2\}$ (6).** By use of the procedure for **4**, 2.00 g (5.35 mmol) of $PtCl_2$(cod) and 3.30 g (5.35 mmol) of **3** yielded 4.88 g (100%) of **6** (mp 185–187 °C) as a white powder. Anal. Calcd for $C_{36}H_{44}Cl_2O_5P_2Pt$: C, 48.86; H, 4.98. Found: C, 48.77; H, 4.97. This material showed three singlets in its ^{31}P NMR spectrum. For **6a**, ^{31}P NMR: δ = 5.47 ppm (major). For **6b**, ^{31}P NMR: δ = 4.50 ppm (minor). For **6c**, ^{31}P NMR: δ = −2.52 ppm (minor). This mixture was chromatographed on silica gel. Elution with 1:1 ethyl acetate–hexanes gave a mixture of **6a** and **6c** (mp 177–179 °C). Anal. Found: C, 48.77; H, 5.00. IR (KBr disk): ν(Pt–Cl) 307, 280 cm^{-1}). Elution with THF gave **6b** (mp 135 °C). Anal. Found: C, 49.14; H, 5.13.

Reaction of *cis*-$PtCl_2\{Ph_2P(CH_2CH_2O)_4CH_2CH_2PPh_2\}$ (5) and $LiBF_4$ in CH_2Cl_2–MeOH. A solution of 0.10 g (0.12 mmol) of **5** and 0.010 g (0.12 mmol) of $LiBF_4$ in 15 mL of a 2:1 dichloromethane–methanol mixture was stirred at ambient temperature for 10 days. The solution was then evaporated to dryness, and the residue, **7**, was treated with acetonitrile-d_3. The mixture was filtered, and a ^{31}P NMR spectrum of the filtrate was recorded. Slow evaporation of this solution yielded colorless crystals of **5**.

Reaction of *cis*-$PtCl_2\{Ph_2P(CH_2CH_2O)_4CH_2CH_2PPh_2\}$ (5) and $LiBF_4$ in CH_2Cl_2–H_2O. A solution of 0.10 g (0.12 mmol) of **5** in 20 mL of dichloromethane and a solution of 1.0 g of $LiBF_4$ in 20 mL of distilled water were combined, and the mixture was stirred for 5 days at ambient temperature. The organic layer was separated and evaporated to dryness to give a white foam. This was dissolved in 3 mL of chloroform-d_1, and the solution was filtered through Celite to remove the small amount of insoluble material. A ^{31}P NMR spectrum was then recorded. This showed the presence of both **5** and a new material **8**. Because **5** was still present, the chloroform-d_1 solution was treated with a solution of 0.12 g of the $LiBF_4$ salt in 3 mL of deionized water, and this mixture was stirred for 24 h. The aqueous solution was then removed, and a ^{31}P NMR spectrum of the chloroform-d_1 solution was again taken. The ^{31}P NMR spectrum indicated that the ratio of **8** to **5** had increased. This procedure was repeated several times, but some **5** was always present. The starting material, **5**, and product, **8**, could not be separated by fractional crystallization.

Reaction of *cis*-$PtCl_2\{Ph_2P(CH_2CH_2O)_4CH_2CH_2PPh_2\}$ (5) and $NaBF_4$ in CH_2Cl_2–H_2O. The preceding procedure was repeated with 0.15 g (0.18 mmol) of **5** and $NaBF_4$. The ^{31}P NMR spectra of the reaction mixtures contained the same resonances as did the ^{31}P NMR spectra of the reaction of **5** with $LiBF_4$ although more **5** was always present.

***trans*-$Pt(CN)_2\{Ph_2P(CH_2CH_2O)_4CH_2CH_2PPh_2\}$ (9).** Solid NaCN (0.012 g, 0.238 mmol) was added to a solution of 0.100 g (0.119 mmol) of **5** in 15 mL of a 2:1 dichloromethane–methanol mixture. The solution was stirred for 18 h and then evaporated to dryness. The residue was treated with chloroform-d_1, and the mixture was filtered. Both ^{31}P and ^{13}C NMR spectra of the filtrate were recorded, and then it was evaporated to dryness. The residue was triturated with both ether and hexanes to give 0.097 g (100%) of **9** as a white powder (mp 72–80 °C). Anal. Calcd for $C_{36}H_{40}N_2O_4P_2Pt$: C, 52.62; H, 4.87. Found: C, 52.76; H, 5.04. IR (KBr disk): ν(CN) 2129 cm^{-1}.

[*cis*-$Pt\{Ph_2P(CH_2CH_2O)_4CH_2CH_2PPh_2$-*P*,*P*′,*O*$\}(H_2O)](BF_4)_2$ (10). A solution of 0.20 g (0.24 mmol) of **5** in 20 mL of a 1:1 dichloromethane–acetonitrile mixture was treated with 0.097 g (0.50 mmol) of solid $AgBF_4$. The cloudy reaction mixture was stirred for 1 h at ambient temperature and then filtered through Celite to yield a clear, colorless solution. This solution was evaporated to dryness to give 0.30 g (100%) of crude **10** as white foam. This material was recrystallized from dichloromethane–hexanes to yield analytically pure **10** as colorless crystals (mp 210–220 °C). Anal. Calcd for $C_{34}H_{42}B_2F_8O_5P_2Pt$: C, 42.47; H, 4.37. Found: C, 42.58; H, 4.40.

Table III. Crystallographic Data for **5**, **6a**, and **10**

compound	5	6a	10
formula	$C_{34}H_{40}Cl_2O_4P_2Pt$	$C_{36}H_{44}Cl_2O_5P_2Pt$	$C_{34}H_{42}B_2F_8O_5P_2Pt$
MW	840.64	884.69	961.36
space group	$P2_1/n$	$P2_1/c$	$P\bar{1}$
a (Å)	12.798 (1)	12.9220 (9)	9.971 (2)
b (Å)	16.4875 (9)	15.5925 (8)	10.293 (2)
c (Å)	16.726 (1)	18.3271 (9)	20.212 (5)
α (deg)			80.92 (2)
β (deg)	104.003 (6)	92.540 (5)	84.92 (2)
γ (deg)			75.48 (1)
V (Å^3)	3424.4	3689.0	1980.3
Z	4	4	2
T (°C)	23	23	23
λ (Å)	1.5418	1.5418	1.5418
d_{calc} (g/cm^3)	1.630	1.592	1.612
absorptn coeff (cm^{-1})	104.050	97.061	81.416
$R(F_o)^a$ (%)	5.48	5.09	5.84
$R_w(F_o)^b$ (%)	7.15	6.63	8.28

$^a R = \sum(|F_o| - |F_c|)/\sum|F_o|)$. $^b R_w = \sum w(|F_o| - |F_c|)^2/\sum|F_o|^2)^{0.5}$.

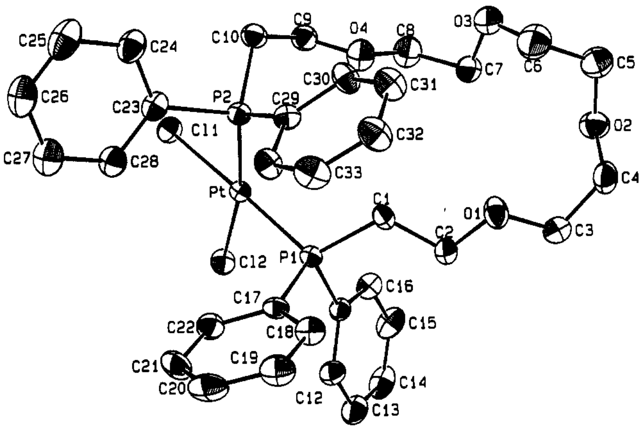

Figure 1. ORTEP[35] drawing of the molecular structure of *cis*-$PtCl_2$-{$Ph_2P(CH_2CH_2O)_4CH_2CH_2PPh_2$} (**5**). The hydrogens are omitted for clarity, and the thermal ellipsoids are drawn at the 25% probability level.

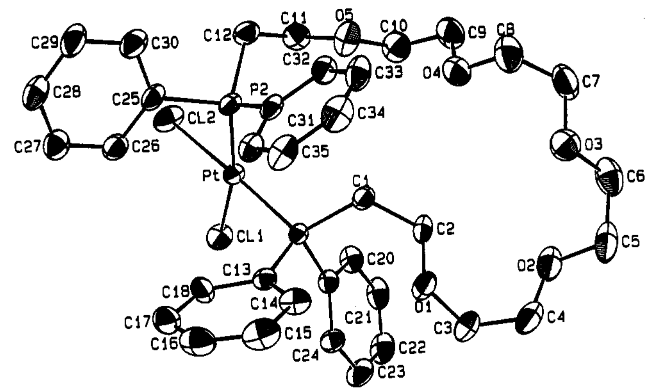

Figure 2. ORTEP[35] drawing of the molecular structure of *cis*-$PtCl_2$-{$Ph_2P(CH_2CH_2O)_5CH_2CH_2PPh_2$} (**6a**). The hydrogens are omitted for clarity, and the thermal ellipsoids are drawn at the 25% probability level.

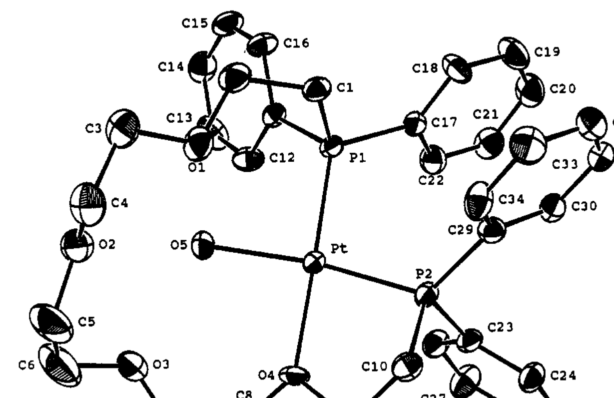

Figure 3. ORTEP[35] drawing of the molecular structure of [*cis*-Pt{Ph_2P-$(CH_2CH_2O)_4CH_2CH_2PPh_2$-*P,P′,O*}($H_2O$)]$(BF_4)_2$ (**10**). The hydrogens are omitted for clarity, and the thermal ellipsoids are drawn at the 25% probability level.

Collection and Reduction of the X-ray Data. Hot, saturated dichloromethane–hexanes solutions of **5**, **6a**, and **10** were slowly cooled to −10 °C to yield crystals of the complexes. Suitable crystals were mounted on glass fibers with epoxy cement. Standard peak search and automatic indexing routines followed by least-squares fits of 25 accurately centered reflections ($2\theta > 25°$) gave the cell constants for each crystal. An Enraf-Nonius CAD-4 diffractometer with Ni-filtered Cu Kα (λ 1.54 18 Å) radiation was used for data collection. Three reflections were remeasured periodically to monitor for decay, and linear decay corrections were applied in each case. The data were processed using the Enraf-Nonius SDP series of programs for **5** and **6a** and on the MolEN series of programs for **10**. Variances were assigned to the I's on the basis of counting statistics with the addition of an instrumental uncertainty term. Lorentz, polarization, and analytical absorption corrections were made to I's and σ^2's for each complex.

Solution and Refinement of the Structure. The cell parameters and systematic absences indicated that the space group of **5** was $P2_1/n$, that of **6a** was $P2_1/c$, and that of **10** was $P\bar{1}$. The positions of the platinum and phosphorus atoms in each of the structures were obtained from the Patterson functions. The remainder of the non-hydrogen atoms in **5** and **6a** were located by Fourier methods. The remaining non-hydrogen atoms in the cationic Pt complex and one of the BF_4^- groups in **10** were located by Fourier methods. The other BF_4^- group was disordered, and all of the atoms could not be located by Fourier methods, but sufficient atoms were located to define three different BF_4^- groups. Each of the structures was refined by a full-matrix least-squares procedure that minimized $w(|F_o| - 1/k|F_c|^2)$, where $w = 1/\sigma^2(F_o)$. All non-H atoms, except for the disordered BF_4^- group in **10**, were refined anisotropically. The three different orientations of the disordered BF_4^- group in **10** were refined as rigid groups with a single average isotropic thermal factor and a variable occupancy using the Crystals program in MolEN. All H atoms in the structures, except for those on the water in **10** which could not be located in the Fourier map, were included in calculated positions (C–H distance of 0.950 Å) with isotropic thermal parameters based upon those of the atoms to which they were attached and were not refined. Data with $I > 3\sigma I$ and with $0.1° < 2\theta < 120°$ (**5**) or $0.1° < 2\theta < 132°$ (**6a** or **10**) were used in the refinement. A secondary extinction correction of the Zachariasen type[23] was made to the data, and the extinction coefficient was refined. In the last stage of each refinement, no parameter varied by more than 0.03 of its standard deviation. The final difference Fourier maps had no interpretable peaks (maximum 2.710 e/Å^3 near the Pt for **5**, −2.033 e/Å^3 near Pt for **6a**, and 1.873 e/Å^3 for **10**). Neutral atom scattering factors were taken from the compilations of Cromer and Weber,[24] and those for H atoms were taken from International Tables

(23) Zachariasen, W. H. *Acta Crystallogr.* **1963**, *16*, 1139.
(24) Cromer, D. T.; Weber, D. T. *Acta Crystallogr.* **1965**, *18*, 104.

Table IV. Fractional Coordinates with esd's for **5**

atom	x	y	z
Pt	0.17897 (2)	0.16821 (2)	0.11279 (2)
C11	0.0419 (2)	0.2251 (2)	0.1672 (1)
C12	0.1791 (2)	0.0575 (1)	0.2003 (1)
P1	0.3129 (2)	0.1090 (1)	0.0690 (1)
P2	0.1465 (2)	0.2741 (1)	0.0244 (1)
O1	0.5902 (5)	0.2136 (5)	0.0428 (4)
O2	0.7434 (6)	0.3408 (4)	0.1179 (5)
O3	0.5369 (6)	0.4457 (5)	0.1109 (6)
O4	0.3424 (6)	0.3723 (5)	0.1317 (4)
C1	0.4150 (7)	0.1796 (5)	0.0482 (6)
C2	0.5294 (7)	0.1509 (6)	0.0654 (7)
C3	0.7023 (8)	0.2042 (7)	0.0731 (7)
C4	0.7556 (7)	0.2816 (8)	0.0594 (7)
C5	0.715 (1)	0.4188 (8)	0.0843 (9)
C6	0.600 (1)	0.4294 (9)	0.0508 (8)
C7	0.5335 (8)	0.3801 (7)	0.1650 (7)
C8	0.4328 (9)	0.3871 (8)	0.1983 (6)
C9	0.2447 (8)	0.3803 (6)	0.1546 (6)
C10	0.1518 (7)	0.3719 (6)	0.0768 (6)
C11	0.3906 (6)	0.0367 (5)	0.1419 (5)
C12	0.3944 (8)	−0.0446 (6)	0.1221 (6)
C13	0.4558 (9)	−0.1002 (7)	0.1785 (8)
C14	0.5118 (9)	−0.0718 (7)	0.2544 (7)
C15	0.5107 (9)	0.0090 (8)	0.2730 (6)
C16	0.4483 (8)	0.0629 (6)	0.2179 (5)
C17	0.2574 (7)	0.0516 (5)	−0.0250 (5)
C18	0.3080 (8)	0.0451 (6)	−0.0896 (6)
C19	0.2589 (9)	0.0065 (7)	−0.1603 (6)
C20	0.161 (1)	−0.0280 (7)	−0.1695 (6)
C21	0.1118 (9)	−0.0258 (7)	−0.1039 (6)
C22	0.1586 (7)	0.0138 (6)	−0.0328 (6)
C23	0.0084 (7)	0.2678 (6)	−0.0380 (5)
C24	−0.0445 (9)	0.3353 (7)	−0.0733 (7)
C25	−0.148 (1)	0.3302 (8)	−0.1270 (7)
C26	−0.1972 (9)	0.2564 (9)	−0.1429 (6)
C27	−0.144 (1)	0.1882 (8)	−0.1063 (6)
C28	−0.0430 (8)	0.1927 (7)	−0.0533 (6)
C29	0.2158 (7)	0.2866 (5)	−0.0566 (5)
C30	0.2957 (8)	0.3454 (6)	−0.0536 (6)
C31	0.3527 (9)	0.3498 (7)	−0.1152 (6)
C32	0.3321 (9)	0.2947 (7)	−0.1804 (6)
C33	0.2517 (9)	0.2393 (7)	−0.1853 (6)
C34	0.1926 (7)	0.2336 (6)	−0.1242 (5)

for X-ray Crystallography.[25] Corrections for the real and imaginary components of anomalous dispersion were taken from the compilations of Cromer and Liberman[26] and were applied to the platinum, chlorine, and phosphorus. Details of the data collection and structure solution procedures are summarized in Table III. The values for the positional parameters for **5**, **6a**, and **10** are given in Tables IV, VI, and VIII, respectively, and selected bond lengths and angles and torsion angles for **5**, **6a**, and **10** are given in Tables V, VII, and IX, respectively. ORTEP drawings of **5**, **6a**, and **10** are given in Figures 1–3, respectively.

Results

***cis*-$PtCl_2\{Ph_2P(CH_2CH_2O)_nCH_2CH_2PPh_2\}$ Complexes.** The reactions of the bis(phosphine)–polyether ligands with $PtCl_2$(cod) under moderately high dilution conditions (eq 1) yield reaction products whose elemental analyses are consistent with the formula *cis*-$PtCl_2\{Ph_2P(CH_2CH_2O)_nCH_2CH_2PPh_2\}$.

$$\begin{gathered}PtCl_2(cod) + \underset{\mathbf{1},\ n=3;\ \mathbf{2},\ n=4;\ \mathbf{3},\ n=5}{Ph_2P(CH_2CH_2O)_nCH_2CH_2PPh_2} \rightarrow \\ \underset{\mathbf{4},\ n=3;\ \mathbf{5},\ n=4;\ \mathbf{6},\ n=5}{cis\text{-}PtCl_2\{Ph_2P(CH_2CH_2O)_nCH_2CH_2PPh_2\}} \quad (1)\end{gathered}$$

The reaction products have been characterized by ^{31}P and ^{13}C NMR spectroscopy, and the data are summarized in Tables I and II. As is the case for the free ligands, the assignments of the ^{13}C NMR resonances due to the methylene carbons that are not adjacent to the phosphorus are conjectural. The assignments in Table II are made on the basis of the relative intensities and positions of the resonances and of their coordination chemical shifts. Single ^{31}P NMR resonances are observed for **4** and **5**, but three different resonances at 5.32 (**6a**), and 4.46 (**6b**), and −2.53 ppm (**6c**) in a ratio of 1.0:0.3:0.15 are observed for **6**. These could be partially separated by chromatography on a silica gel column. Elution with a 1:1 ethyl acetate–hexanes mixture gave a mixture of **6a** and **6c** and then elution with THF gave pure **6b**. The elemental analyses of the mixture and both fractions are nearly identical and are consistent with the empirical formula shown in eq 1.

(25) *International Tables for X-ray Crystallography*; Kynoch Press: Birmingham, UK, 1974; Vol. IV, p 72.
(26) Cromer, D. T.; Liberman, D. J. *J. Chem. Phys.* **1970**, *53*, 1891.

Table V. Selected Bond Distances (Å) and Angles (deg) with esd's for **5**

Bond Distances

Pt–C11	2.357 (2)	P2–C23	1.826 (8)	O4–C8	1.42 (1)
Pt–C12	2.340 (2)	P2–C29	1.801 (9)	O4–C9	1.40 (1)
Pt–P1	2.245 (2)	O1–C2	1.40 (1)	C1–C2	1.50 (1)
Pt–P2	2.261 (2)	O1–C3	1.41 (1)	C3–C4	1.49 (2)
P1–C1	1.85 (1)	O2–C4	1.42 (1)	C5–C6	1.45 (2)
P1–C11	1.819 (8)	O2–C5	1.42 (1)	C7–C8	1.53 (2)
P1–C17	1.825 (8)	O3–C6	1.46 (2)	C9–C10	1.54 (1)
P2–C10	1.83 (1)	O3–C7	1.42 (1)		

Bond Angles

C11–Pt–C12	87.53 (8)	C4–O2–C5	114.4 (9)
C11–Pt–P1	176.05 (7)	C6–O3–C7	114.0 (9)
C11–Pt–P2	84.78 (8)	C8–O4–C9	112.4 (8)
C12–Pt–P1	88.84 (7)	P1–C1–C2	117.9 (6)
C12–Pt–P2	169.76 (7)	O1–C2–C1	107.2 (8)
P1–Pt–P2	99.01 (8)	O1–C3–C4	108.3 (8)
Pt–P1–C1	114.7 (3)	O2–C4–C3	110.6 (9)
Pt–P1–C11	113.8 (3)	O2–C5–C6	114 (1)
Pt–P1–C17	109.7 (3)	O3–C6–C5	116 (1)
Pt–P2–C10	112.8 (3)	O3–C7–C8	109.5 (9)
Pt–P2–C23	109.2 (3)	O4–C8–C7	107.5 (9)
Pt–P2–C29	122.3 (3)	O4–C9–C10	108.6 (8)
C2–O1–C3	114.0 (7)	P2–C10–C9	114.5 (7)

Torsion Angles

P2–Pt–P1–C1	43.5 (5)	C5–C6–O3–C7	66 (1)
Pt–P1–C1–C2	146.2 (7)	C6–O3–C7–C8	−156 (1)
P1–C1–C2–O1	178.4 (6)	O3–C7–C8–O4	69 (1)
C1–C2–O1–C3	−165.6 (8)	C7–C8–O4–C9	177.7 (9)
C2–O1–C3–C4	−168.8 (8)	C8–O4–C9–C10	174.2 (8)
O1–C3–C4–O2	76 (1)	O4–C9–C10–P2	61 (1)
C3–C4–O2–C5	136 (1)	C9–C10–P2–Pt	−41.7 (8)
C4–O2–C5–C6	85 (1)	C10–P2–Pt–P1	126.1 (3)
O2–C5–C6–O3	80 (1)		

The X-ray crystal structures of **5** and **6a** have been determined. The results are presented in Tables IV and V for **5** and Tables VI and VII for **6a**. ORTEP drawings of **5** and **6a** are shown in Figures 1 and 2, respectively. This data will be introduced in the appropriate places in the Discussion section that follows.

Reactions of *cis*-$PtCl_2\{Ph_2P(CH_2CH_2O)_4CH_2CH_2PPh_2\}$ (5) with Alkali Metal Salts. The reaction of **5** and $LiBF_4$ in a 1:1 ratio in a dichloromethane–methanol mixture yielded a new complex, **7**, that was insoluble in chloroform-d_1 and soluble in acetonitrile-d_3, in contrast to **5**, which was soluble in chloroform-d_1 and insoluble in acetonitrile-d_3. Attempts to recrystallize **7** from a dichloromethane–methanol mixture yielded only **5**, and attempts to recrystallize **7** from a dichloromethane–hexanes mixture caused $LiBF_4$ to precipitate. Slow evaporation of the acetonitrile-d_3 solution also gave **5**.

The reactions of **5** with MBF_4 salts (M = Li, Na) in chloroform-d_1–water mixtures yielded a different product, **8**. Unfortunately, even when a large excess of the MBF_4 salt was used, some **5** remained in equilibrium with **8**, and the two materials could not be separated. The ratio of **8** to **5** was always larger when M = Li than when M = Na for solutions that were treated similarly.

The reaction of **5** with NaCN in a 1:2 molar ratio gave a quantitative yield of *trans*-$Pt(CN)_2\{Ph_2P$-

Table VI. Fractional Coordinates with esd's for **6a**

atom	x	y	z
Pt	0.25605 (2)	0.04261 (2)	0.14310 (2)
Cl1	0.3082 (2)	0.1854 (1)	0.1508 (1)
Cl2	0.1980 (2)	0.0725 (2)	0.0222 (1)
P1	0.3131 (1)	0.0218 (1)	0.2595 (1)
P2	0.2147 (2)	−0.0938 (1)	0.1134 (1)
O1	0.3215 (5)	−0.0357 (4)	0.4306 (3)
O2	0.1759 (7)	−0.0394 (4)	0.5483 (4)
O3	0.0384 (6)	−0.1640 (5)	0.4949 (4)
O4	−0.0090 (5)	−0.1489 (6)	0.3358 (4)
O5	−0.0092 (6)	−0.0952 (5)	0.1905 (4)
C1	0.2341 (7)	−0.0513 (5)	0.3128 (4)
C2	0.2240 (7)	−0.0317 (5)	0.3933 (4)
C3	0.3291 (9)	0.0072 (9)	0.4987 (5)
C4	0.286 (1)	−0.0410 (9)	0.5584 (6)
C5	0.127 (1)	−0.0987 (8)	0.5936 (6)
C6	0.0227 (9)	−0.1178 (7)	0.5590 (7)
C7	−0.0532 (8)	−0.1910 (9)	0.4585 (7)
C8	−0.031 (1)	−0.2197 (8)	0.3845 (7)
C9	−0.0981 (7)	−0.1169 (9)	0.3005 (7)
C10	−0.0704 (8)	−0.0524 (7)	0.2432 (7)
C11	0.0033 (7)	−0.0509 (6)	0.1259 (6)
C12	0.0786 (7)	−0.1016 (6)	0.0793 (5)
C13	0.4423 (6)	−0.0229 (5)	0.2602 (4)
C14	0.4796 (7)	−0.0802 (5)	0.3122 (6)
C15	0.5752 (8)	−0.1193 (6)	0.3038 (7)
C16	0.6308 (7)	−0.1050 (7)	0.2458 (7)
C17	0.5992 (8)	−0.0440 (7)	0.1925 (6)
C18	0.5030 (6)	−0.0017 (6)	0.2014 (5)
C19	0.3199 (6)	0.1173 (5)	0.3151 (4)
C20	0.2312 (7)	0.1685 (5)	0.3210 (5)
C21	0.2333 (8)	0.2371 (6)	0.3704 (6)
C22	0.321 (1)	0.2544 (6)	0.4129 (6)
C23	0.4080 (9)	0.2054 (6)	0.4063 (6)
C24	0.4093 (7)	0.1372 (5)	0.3584 (5)
C25	0.2912 (7)	−0.1299 (5)	0.0382 (4)
C26	0.3877 (8)	−0.0937 (6)	0.0276 (5)
C27	0.4525 (8)	−0.1287 (6)	−0.0243 (5)
C28	0.4216 (9)	−0.1972 (6)	−0.0633 (5)
C29	0.3259 (9)	−0.2325 (7)	−0.0551 (5)
C30	0.2601 (9)	−0.2000 (6)	−0.0028 (5)
C31	0.2396 (7)	−0.1832 (5)	0.1756 (4)
C32	0.1593 (7)	−0.2251 (5)	0.2109 (5)
C33	0.1842 (8)	−0.2943 (6)	0.2569 (5)
C34	0.2855 (9)	−0.3221 (6)	0.2665 (6)
C35	0.3643 (8)	−0.2817 (6)	0.2331 (5)
C36	0.3409 (7)	−0.2125 (5)	0.1877 (5)

$(CH_2CH_2O)_4CH_2CH_2PPh_2\}$ (**9**) (eq 2). The small $|^1J(PtP)|$ of 2323 Hz and the presence of a single IR absorption at 2128 cm^{-1} for the cyanide ligands indicate that ligands are trans in **9**.

$$\underset{\mathbf{5}}{cis\text{-}PtCl_2\{Ph_2P(CH_2CH_2O)_4CH_2CH_2PPh_2\}} + 2NaCN \rightarrow \underset{\mathbf{9}}{trans\text{-}Pt(CN)_2\{Ph_2P(CH_2CH_2O)_4CH_2CH_2PPh_2\}} \quad (2)$$

$[cis\text{-}Pt\{Ph_2P(CH_2CH_2O)_4CH_2CH_2PPh_2\text{-}P,P',O\}(H_2O)](BF_4)_2$ (10). The reaction of **5** with $AgBF_4$ gave a quantitative yield of **10** (eq 3).

$$\underset{\mathbf{5}}{cis\text{-}PtCl_2\{Ph_2P(CH_2CH_2O)_4CH_2CH_2PPh_2\}} + 2AgBF_4 \xrightarrow[CH_3CN]{CH_2Cl_2} \underset{\mathbf{10}}{[cis\text{-}Pt\{Ph_2P(CH_2CH_2O)_4CH_2CH_2PPh_2\text{-}P,P',O\}(H_2O)](BF_4)_2} \quad (3)$$

In chloroform-d_1, **10** exhibits two broad ^{31}P NMR resonances of approximately equal intensities at 22.71 ($|^1J(PtP)| = 4143$ Hz) and 1.50 ppm ($|^1J(PtP)| = 4619$ Hz). When **10** is dissolved in acetonitrile-d_3, a new complex, **11**, is formed. This complex has a single, slightly broadened, ^{31}P NMR resonance at 0.56 ppm ($|^1J(PtP)| = 3767$ Hz), **11**. The ^{13}C NMR spectrum of **11** is unusual in that all of the resonances normally coupled to phosphorus are doublets rather than apparent quintets.

The X-ray crystal structure of **10** has been determined. The results are presented in Tables VIII and IX. An ORTEP drawing of **10** is shown in Figure 3. These data will be introduced in the appropriate places in the Discussion section that follows.

Table VII. Selected Bond Distances (Å) and Angles (deg) with esd's for **6a**

Bond Distances					
Pt–Cl1	2.330 (2)	P2–C31	1.821 (7)	O5–C10	1.44 (1)
Pt–Cl2	2.354 (2)	O1–C2	1.41 (1)	O5–C11	1.39 (1)
Pt–P1	2.250 (2)	O1–C3	1.41 (1)	C1–C2	1.52 (1)
Pt–P2	2.255 (2)	O2–C4	1.43 (2)	C3–C4	1.46 (2)
P1–C1	1.840 (8)	O2–C5	1.41 (1)	C5–C6	1.49 (2)
P1–C13	1.809 (7)	O3–C6	1.40 (1)	C7–C8	1.47 (2)
P1–C19	1.804 (8)	O3–C7	1.40 (1)	C9–C10	1.51 (2)
P2–C12	1.84 (1)	O4–C8	1.46 (2)	C11–C12	1.54 (1)
P2–C25	1.821 (9)	O4–C9	1.39 (1)		

Bond Angles			
Cl1–Pt–Cl2	86.96 (9)	C2–O1–C3	115.7 (7)
Cl1–Pt–P1	89.91 (7)	C4–O2–C5	112.5 (9)
Cl1–Pt–P2	169.06 (8)	C6–O3–C7	113.9 (9)
Cl2–Pt–P1	176.84 (8)	C8–O4–C9	112.2 (9)
Cl2–Pt–P2	84.13 (7)	C10–O5–C11	115.5 (8)
P1–Pt–P2	99.03 (6)	P1–C1–C2	117.7 (6)
Pt–P1–C1	115.2 (3)	O1–C2–C1	110.5 (7)
Pt–P1–C13	109.0 (3)	O1–C3–C4	114 (1)
Pt–P1–C19	114.9 (3)	O2–C4–C3	108 (1)
C1–P1–C13	106.9 (4)	O2–C5–C6	107.5 (9)
C1–P1–C19	103.1 (4)	O3–C6–C5	107 (1)
C13–P1–C19	107.1 (3)	O3–C7–C8	110 (1)
Pt–P2–C12	110.9 (3)	O4–C8–C7	113 (1)
Pt–P2–C25	110.1 (3)	O4–C9–C10	110.3 (9)
Pt–P2–C31	122.5 (2)	O5–C10–C9	108.1 (9)
C12–P2–C25	105.4 (4)	O5–C11–C12	108.5 (8)
C12–P2–C31	107.5 (4)	P2–C12–C11	113.2 (6)
C25–P2–C31	98.7 (4)		

Torsion Angles			
P2–Pt–P1–C1	−42.8 (3)	C6–O3–C7–C8	166 (1)
Pt–P1–C1–C2	−145.0 (6)	O3–C7–C8–O4	−73 (1)
P1–C1–C2–O1	−62.5 (8)	C7–C8–O4–C9	89 (1)
C1–C2–O1–C3	−160.3 (8)	C8–O4–C9–C10	−172 (1)
C2–O1–C3–C4	80 (1)	O4–C9–C10–O5	61 (1)
O1–C3–C4–O2	−73 (1)	C9–C10–O5–C11	−166.2 (8)
C3–C4–O2–C5	−167 (1)	C10–O5–C11–C12	174.7 (8)
C4–O2–C5–C6	−157 (1)	O5–C11–C12–P2	−74.3 (8)
O2–C5–C6–O3	69 (1)	C11–C12–P2–Pt	44.7 (7)
C5–C6–O3–C7	−176 (1)	C12–P2–Pt–P1	−124.5 (3)

Discussion

Solid-State and Solution Structures of the $cis\text{-}PtCl_2\{Ph_2P(CH_2CH_2O)_nCH_2CH_2PPh_2\}$ Complexes. The solid-state and solution structures of these metallacrown ether complexes are of interest because they provide insight into the ability of these complexes to coordinate to hard metal cations. The X-ray crystal structures of **5** and **6a** are similar. In each, the platinum has a cis square planar coordination geometry (Pt, Cl1, Cl2, P1, and P2 are within 0.10 (2) Å of their least-squares plane in **5** and within 0.08 (3) Å their least-squares plane in **6a**). The P1–Pt–P2 angles are larger than 90° and the Cl1–Pt–P2, Cl2–Pt–P1, and Cl1–Pt–Cl2 angles smaller than 90°. The distortions from square planar geometry in **5** and **6a** are less than those in $cis\text{-}PdCl_2\{Ph_2P(CH_2CH_2O)_2CH_2CH_2PPh_2\}$ (**12**) (P–Pd–P angle, 105.4 (1)°; Cl–Pd–P angles, 82.5 (1), 84.1 (1)°; Cl–Pd–Cl angle, 88.1 (1)°).[3] The smaller distortions in **5** and **6a** are consistent with the longer metal–phosphorus bonds in **5** and **6a**, which reduce the steric interactions between the bulky diphenylphosphino groups.

The conformations of the metallacrown ether rings are the most interesting features in these structures. As in **12**[3] and $cis\text{-}Mo(CO)_4\{Ph_2P(CH_2CH_2O)_3CH_2CH_2PPh_2\}$,[8] the chelate rings are asymmetric due to different rotations of the diphenylphosphino groups about the platinum–phosphorus bonds. These rotations are very similar in **5** and **6a**, as indicated by the similar torsion angles. The oxygens in the chelate rings in **5** and **6a** are relatively planar (deviations from the least-squares plane of the oxygens +0.200 (7), −0.330 (8), +0.386 (9), and −0.257 (7) Å in **5**; +0.399 (6), −0.648 (7), +0.354 (8), +0.176 (8), and −0.281 (8) Å in **6a**). This behavior is similar to that observed for benzo-18-crown-6

Table VIII. Fractional Coordinates with esd's for **10**

atom	x	y	z
Pt	0.18355 (3)	0.19224 (3)	0.23791 (1)
P1	0.1829 (2)	0.3390 (2)	0.30772 (9)
P2	−0.0426 (2)	0.2235 (2)	0.2310 (1)
O1	0.3780 (7)	0.4252 (7)	0.1794 (4)
O2	0.5772 (8)	0.2354 (8)	0.1146 (4)
O3	0.4978 (8)	−0.0136 (8)	0.1415 (4)
O4	0.1868 (6)	0.0573 (5)	0.1657 (3)
O5	0.4012 (5)	0.1605 (6)	0.2244 (3)
C1	0.1913 (8)	0.5039 (7)	0.2602 (4)
C2	0.332 (1)	0.5138 (9)	0.2256 (5)
C3	0.496 (1)	0.457 (1)	0.1397 (6)
C4	0.529 (1)	0.371 (1)	0.0844 (6)
C5	0.599 (2)	0.139 (2)	0.0668 (7)
C6	0.611 (2)	0.008 (2)	0.0963 (9)
C7	0.399 (1)	−0.068 (1)	0.1160 (6)
C8	0.284 (1)	−0.0723 (9)	0.1669 (5)
C9	0.060 (1)	0.066 (1)	0.1329 (5)
C10	−0.0407 (9)	0.200 (1)	0.1434 (4)
C11	0.3275 (8)	0.2880 (7)	0.3602 (4)
C12	0.393 (1)	0.1515 (9)	0.3775 (4)
C13	0.497 (1)	0.114 (1)	0.4240 (6)
C14	0.535 (1)	0.209 (1)	0.4536 (5)
C15	0.469 (1)	0.341 (1)	0.4385 (5)
C16	0.3687 (9)	0.3830 (9)	0.3921 (5)
C17	0.0397 (8)	0.3655 (8)	0.3691 (4)
C18	−0.036 (1)	0.4893 (9)	0.3830 (5)
C19	−0.134 (1)	0.498 (1)	0.4350 (6)
C20	−0.162 (1)	0.387 (1)	0.4749 (6)
C21	−0.086 (1)	0.261 (1)	0.4622 (6)
C22	0.014 (1)	0.252 (1)	0.4100 (5)
C23	−0.1166 (8)	0.0912 (7)	0.2776 (5)
C24	−0.2467 (9)	0.0840 (9)	0.2650 (5)
C25	−0.3004 (9)	−0.023 (1)	0.2975 (6)
C26	−0.219 (1)	−0.126 (1)	0.3410 (7)
C27	−0.090 (1)	−0.118 (1)	0.3527 (6)
C28	−0.0350 (9)	−0.0109 (9)	0.3217 (5)
C29	−0.1599 (9)	0.3866 (8)	0.2394 (5)
C30	−0.2604 (9)	0.4031 (9)	0.2910 (5)
C31	−0.3440 (9)	0.529 (1)	0.2955 (6)
C32	−0.329 (1)	0.640 (1)	0.2499 (7)
C33	−0.228 (1)	0.624 (1)	0.1984 (7)
C34	−0.145 (1)	0.496 (1)	0.1930 (6)
B1	0.335 (1)	0.792 (1)	0.3661 (5)
F1	0.2505 (6)	0.8780 (6)	0.4058 (3)
F2	0.4248 (8)	0.6937 (8)	0.4047 (4)
F3	0.2588 (8)	0.7300 (7)	0.3329 (5)
F4	0.4041 (8)	0.8650 (7)	0.3182 (4)
B2	0.120 (3)	0.735 (2)	0.057 (1)
F5	0.074 (3)	0.661 (3)	0.014 (2)
F6	0.029 (3)	0.736 (3)	0.114 (2)
F7	0.258 (3)	0.671 (3)	0.073 (2)
F8	0.114 (3)	0.869 (3)	0.025 (2)
B2′	0.084 (3)	0.714 (2)	0.077 (1)
F5′	0.096 (3)	0.576 (3)	0.073 (2)
F6′	0.053 (3)	0.738 (3)	0.143 (2)
F7′	0.208 (3)	0.749 (3)	0.053 (2)
F8′	−0.028 (3)	0.795 (3)	0.040 (2)
B2″	0.096 (3)	0.688 (2)	0.049 (1)
F5″	−0.035 (3)	0.661 (3)	0.051 (2)
F6″	0.133 (3)	0.687 (3)	0.115 (2)
F7″	0.192 (3)	0.587 (3)	0.019 (2)
F8″	0.094 (3)	0.816 (3)	0.012 (2)

in which the oxygens are all within 0.184 Å of the least-squares plane.[27]

Because the oxygens in the metallacrown ether rings in **5** and **6a** are relatively planar, rough estimates of the cavity sizes in the complexes can be obtained from the average distances between oxygens that could serve as trans ligands to a cation. In **5**, these would be O1–O3 and O2–O4 with an average distance of 4.66 Å. In **6a**, the trans oxygens are less certain but could be O1–O4 and O2–O5 with an average distance of 5.32 Å. The average trans oxygen–oxygen distance in **5** is too small to accommodate Na^+ but should easily accommodate Li^+, while that in **6a** is large enough to accommodate Na^+.[28] These results are consistent with the cation selectivities exhibited by the *cis*-$Mo(CO)_4\{Ph_2P(CH_2CH_2O)_nCH_2CH_2PPh_2\}$ (n = 4, 5) metallacrown ethers (n = 4 complex strongly coordinates Li^+ and weakly coordinates Na^+; n = 5 complex weakly coordinates Li^+ and strongly coordinates Na^+).[8]

The average solution structures of the *cis*-$PtCl_2\{Ph_2P(CH_2CH_2O)_nCH_2CH_2PPh_2\}$ complexes are different from the solid-state conformations. Single ^{31}P NMR resonances are observed for **4**, **5**, and **6a** (major component), and the ^{31}P NMR resonances of the three complexes have very similar chemical shifts and $|^1J(PtP)|$'s. These similarities and the fact that both **5** and **6a** are monomeric, as shown by their X-ray crystal structures, suggest that all of these complexes are monomeric, cis square planar complexes. This conclusion is further supported by the similarities in their ^{13}C NMR spectra. The metallacrown ethers rings in these complexes appear to be fluxional because a single ^{31}P NMR resonance is observed for each complex and a single ^{13}C NMR resonance is observed for each set of equivalent methylenes in the complexes.

The nature of **6b** is less clear. The similar ^{31}P NMR chemical shifts and $|^1J(PtP)|$'s of **6a** and **6b** indicate that the platinum has a cis square planar $PtCl_2P_2$ geometry in each complex. The complexes also have nearly identical elemental analyses, which indicates that they have the same empirical formulas. However, the very different chemical shifts of the ^{13}C NMR resonances of the phenyl and aliphatic carbons in the two complexes suggest that the $Ph_2P(CH_2CH_2O)_5CH_2CH_2PPh_2$ ligands have very different conformations in **6a** and **6b**. A possible explanation for this is that **6b** is an oligomer of **6a**; however, we have been unable to obtain a sufficient quantity of pure **6b** in order to be able to determine its molecular weight and prove this point.

Table IX. Selected Bond Distances (Å) and Angles (deg) with esd's for **10**

Bond Distances

Pt–P1	2.223 (2)	P2–C23	1.806 (8)	O4–C8	1.44 (1)
Pt–P2	2.211 (2)	P2–C29	1.813 (8)	O4–C9	1.46 (1)
Pt–O4	2.162 (6)	O1–C2	1.38 (1)	C1–C2	1.54 (1)
Pt–O5	2.111 (5)	O1–C3	1.44 (1)	C3–C4	1.49 (2)
P1–C1	1.831 (8)	O2–C4	1.41 (1)	C5–C6	1.36 (2)
P1–C11	1.787 (8)	O2–C5	1.46 (2)	C7–C8	1.48 (2)
P1–C17	1.803 (8)	O3–C6	1.43 (2)	C9–C10	1.52 (1)
P2–C10	1.824 (9)	O3–C7	1.42 (2)		

Bond Angles

P1–Pt–P2	99.31 (7)	C6–O3–C7	116 (1)
P1–Pt–O4	176.9 (2)	Pt–O4–C8	122.7 (6)
P1–Pt–O5	89.2 (2)	Pt–O4–C9	119.1 (5)
P2–Pt–O4	81.3 (2)	C8–O4–C9	113.5 (7)
P2–Pt–O5	168.9 (2)	P1–C1–C2	116.1 (5)
O4–Pt–O5	89.8 (2)	O1–C2–C1	113.1 (9)
Pt–P1–C1	110.1 (3)	O1–C3–C4	108 (1)
Pt–P1–C11	113.1 (3)	O2–C4–C3	106.9 (9)
Pt–P1–C17	116.8 (3)	O2–C5–C6	114 (1)
Pt–P2–C10	97.6 (3)	O3–C6–C5	115 (1)
Pt–P2–C23	115.2 (3)	O3–C7–C8	109 (1)
Pt–P2–C29	121.0 (3)	O4–C8–C7	111.7 (8)
C2–O1–C3	110.5 (8)	O4–C9–C10	108.0 (9)
C4–O2–C5	112.6 (9)	P2–C10–C9	108.8 (6)

Torsion Angles

P2–Pt–P1–C1	−92.1 (3)	C5–C6–O3–C7	−100 (2)
Pt–P1–C1–C2	−74.0 (7)	C6–O3–C7–C8	−175 (1)
P1–C1–C2–O1	60 (1)	O3–C7–C8–O4	81 (1)
C1–C2–O1–C3	−165.6 (8)	C7–C8–O4–C9	−103 (1)
C2–O1–C3–C4	−169.0 (8)	C8–O4–C9–C10	172.5 (7)
O1–C3–C4–O2	−68 (1)	O4–C9–C10–P2	−45.8 (9)
C3–C4–O2–C5	−174 (1)	C9–C10–P2–Pt	−52.8 (7)
C4–O2–C5–C6	−164 (1)	C10–P2–Pt–P1	−144.9 (3)
O2–C5–C6–O3	55 (2)		

(27) Bright, D.; Truter, M. R. *J. Chem. Soc. B* **1970**, 1544.

(28) Bajaj, A. V.; Poonia, N. S. *Coord. Chem. Rev.* **1988**, *87*, 55, and references therein.

The nature of **6c** is even more difficult to determine because it is only observed as a minor product in solutions of **6a**, and thus its ^{13}C NMR spectrum cannot be obtained. The large $|^1J(PtP)|$ indicates the phosphine ligands are still cis, but the broad, upfield ^{31}P NMR resonance of this material suggests that one or both of the chloride ligands may have been lost. This is supported by the similarities of the ^{31}P NMR spectra of **6c** and **11** (see following discussion on the nature of **11**). However, if **6c** is cationic, it is surprising that it would coelute with the neutral **6a**. One possibility is that these complexes are in equilibrium in solution, but only **6a** exists in the solid state.

Reactions of *cis*-$PtCl_2\{Ph_2P(CH_2CH_2O)_4CH_2CH_2PPh_2\}$ (5) with Alkali Metal Salts. Previous studies of *cis*-$Mo(CO)_4\{Ph_2P(CH_2CH_2O)_nCH_2CH_2PPh_2\}$ (n = 4, 5) metallacrown ethers have demonstrated that these complexes can coordinate alkali metal cations and that the strength of the coordination depends on the size of the cavity in the metallacrown ether.[8,13] The X-ray crystal structures of **5** and **6a** indicate that these complexes should also be able to coordinate alkali metal cations. Unfortunately, replacing the octahedral *cis*-$Mo(CO)_4$ group with a square planar *cis*-$PtCl_2$ group greatly complicates the reactions of the metallacrown ethers with alkali metal salts.

The reaction of **5** with $LiBF_4$ in a dichloromethane–methanol mixture yields a new complex, **7**, that is dichloromethane insoluble and acetonitrile soluble, unlike **5**, which is dichloromethane soluble and acetonitrile insoluble. Both the differences in the solubilities and in the chemical shifts of the ^{31}P NMR resonances of **5** and **7** suggest that **7** is a $LiBF_4$ complex of **5**. However, attempts to recrystallize **7** from either acetonitrile or a dichloromethane–methanol mixture yield only the starting material, **5**, while attempts to recrystallize **7** from a dichloromethane–hexanes mixture initially yield $LiBF_4$. This behavior appears to be due to the equilibrium shown in eq 4, which shifts toward the reactants to

$$\underset{\mathbf{5}}{cis\text{-}PtCl_2\{Ph_2P(CH_2CH_2O)_4CH_2CH_2PPh_2\}} + LiBF_4 \rightleftharpoons \underset{\mathbf{7}}{[cis\text{-}PtCl_2\{Ph_2P(CH_2CH_2O)_4CH_2CH_2PPh_2\}Li]BF_4}\ (?) \quad (4)$$

allow **5** to precipitate from polar solvents such as methanol or acetonitrile and $LiBF_4$ to precipitate from nonpolar solvents such as hexanes.

The reactions of **5** with MBF_4 salts (M^+ = Li^+, Na^+) in two-phase chloroform-d_1–water mixtures yield a different complex, **8**, which has two phosphines in different chemical environments (^{31}P NMR: δ 4.67 ppm, d, dd, $|^1J(PtP)|$ = 4237 Hz, $|^2J(PP')|$ = 15 Hz; δ 36.17 ppm, d, dd, $|^1J(PtP)|$ = 3691 Hz, $|^2J(PP')|$ = 15 Hz). The similarity of the ^{31}P NMR spectrum of **8** to that of $[cis\text{-}PtCl(Ph_2PCH_2C_4H_7O\text{-}P)(Ph_2PCH_2C_4H_7O\text{-}P,O)][PF_6]$[29] ($^{31}P$ NMR: δ 4.5 ppm, d, dd, $|^1J(PtP)|$ = 4048 Hz, $|^2J(PP')|$ = 17 Hz; δ 32.1 ppm, d, dd, $|^1J(PtP)|$ = 3662 Hz, $|^2J(PP')|$ = 17 Hz) and the fact that the NMR spectrum of **8** is the same regardless of whether M^+ is Li^+ or Na^+ suggest that **8** is $[cis\text{-}PtCl\{Ph_2P(CH_2CH_2O)_4CH_2CH_2PPh_2\text{-}P,P',O\}](X)$ (X = BF_4 or Cl). The apparent lack of alkali metal cation coordination is not surprising because one of the ether oxygens is unavailable for coordination and the complex is cationic.

The ease of chloride displacement from **5** is also demonstrated by the quantitative reaction of **5** with NaCN to form *trans*-$Pt(CN)_2\{Ph_2P(CH_2CH_2O)_4CH_2CH_2PPh_2\text{-}P,P'\}$ (**9**). The facile displacement of the chloride ligands from **5** is consistent with the results of Okano et al.[30] These authors noted that $PdCl_2$(phosphinocrown ether) complexes readily underwent halide-exchange reactions with NaBr and NaI in chloroform, whereas $PdCl_2(PPh_3)_2$ took nearly 10 h for 30% exchange. They suggested that this was due to the ability of the crown ether to facilitate the separation of ion pairs to initiate the chloride displacement. This indicates that alkali metal cation coordination by *cis*-$PtCl_2\{Ph_2P(CH_2CH_2O)_4CH_2CH_2PPh_2\text{-}P,P'\}$ metallacrown ethers will only occur under conditions that do not favor loss of the chloride ligands.

Solid-State and Solution Structures of $[cis\text{-}Pt\{Ph_2P(CH_2CH_2O)_nCH_2CH_2PPh_2\}(H_2O)](BF_4)_2$. The unusual ^{31}P NMR spectrum of **10** and the presence of a molecule of water in this complex suggest that it might have an unusual structure. This is indeed the case in the solid state. The platinum is coordinated to both phosphine groups, an adjacent ether oxygen, and a water oxygen in a distorted cis square planar arrangement. The P1–Pt–P2 bond angle (99.31 (7)°) is similar to those in **5** (99.01 (8)°) and **6a** (99.03 (6)°), and the O4–Pt–O5 angle (89.8 (2)°) is similar to the Cl1–Pt–Cl2 angles in **5** (87.53 (8)°) and **6a** (86.96 (9)°). All the atoms in the platinum coordination sphere lie within 0.07 (1) Å of the least-squares plane through the Pt, P1, P2, O4, and O5. The coordination of the water rather than a second ether oxygen to platinum is surprising because neither water nor ethers strongly coordinate to platinum, and the chelate effect should favor the coordination of another ether oxygen. The preferential coordination of water appears to be due to the formation of hydrogen bonds between two other ether oxygens, O1 and O3, and the protons on water. These result in short oxygen–oxygen distances between O5 and O1 (2.597 Å) and O5 and O3 (2.691 Å) and are consistent with the O1–O5–O3 angle of 118°. Similar coordination of a water has been reported in only two other complexes. In one, $[cis\text{-}Rh(CO)(H_2O)\{Ph_2P(CH_2CH_2O)_3CH_2CH_2PPh_2\}](PF)_6$, the water is coordinated to a rhodium(I) and hydrogen bonded to two of three ether oxygens in the metallacrown ether.[1,2] The distances between hydrogen-bonded oxygens in this complex, 2.67 (1) and 2.69 (1) Å, are similar to that between O5 and O3 in **10**. In the other, the water is coordinated to a rhodium(III) and is hydrogen bonded to the ether oxygens of a metallacrown ether with water oxygen–ether oxygen distances of 2.986 (6) and 3.128 (6) Å. These longer distances suggest that the hydrogen bonding is significantly weaker in this complex than in **10**.[31]

The platinum–oxygen bond lengths in **10** (Pt–O5 = 2.111 (5) Å and Pt–O4 = 2.162 (6) Å) are similar to those reported in other platinum(II) complexes with chelating phosphine/ether ligands (2.142 (4) Å for $[cis\text{-}PtCl(Ph_2PCH_2C_4H_7O\text{-}P)(Ph_2PCH_2C_4H_7O\text{-}P,O)][PF_6]$[29]) and longer than those reported for platinum(II) complexes with chelating phosphine/alkoxide ligands (2.023 (5) Å in $Pt(Ph_2PCH_2CMe_2O\text{-}P,O)_2$[32] and 2.039 (5) Å in $Pt(Ph_2PCH_2CH_2O\text{-}P,O)_2$[33]). This is consistent with the weaker bonding of the ether and water oxygens to platinum compared to the bonding of the alkoxy oxygens to platinum.

The conformation of the metallacrown ether rings in **10** is significantly different from the conformations of the rings in **5** and **6a** because the coordination of O4 to Pt and the hydrogen bonding of O1 and O3 to the water in **10** forces the ring to wrap around the platinum. In **5** and **6a**, the rings extend away from the platinum, and no interaction with the chloride ligands is observed. These differences illustrate the flexibility of the metallacrown ether ring which allows it to adopt a variety of different conformations.

The average solution structure of **10** is different from its solid-state structure. In chloroform-d_1, the ^{31}P NMR spectrum of **10** contains two broad resonances. The downfield resonance is due to phosphorus in five-membered chelate rings formed by coordination of an adjacent ether oxygen, and the upfield resonance is due to phosphorus in eight-membered chelate rings formed by the coordination of a nonadjacent ether oxygen. The resonances are broad due to slow exchange of oxygens at the platinum. This is in contrast to the solid-state structure where only five-membered chelate rings are observed. The ^{31}P NMR spectrum does not provide any information as to whether a water is coordinated to the platinum in **10** in solution.

(29) Alcock, N. W.; Platt, A. W. G.; Pringle, P. G. *J. Chem. Soc., Dalton Trans.* **1989**, 2069.
(30) Okano, T.; Iwahara, M.; Suzuki, T.; Konishi, H.; Kiji, J. *Chem. Lett.* **1986**, 1467.
(31) Ferguson, G.; Matthes, K.; Parker, D. *Angew. Chem., Int. Ed. Engl.* **1987**, *26*, 1162.
(32) Alcock, N. W.; Platt, A. W. G.; Pringle, P. G. *J. Chem. Soc., Dalton Trans.* **1987**, 2273.
(33) Alcock, N. W.; Platt, A. W. G.; Pringle, P. G. *J. Chem. Soc., Dalton Trans.* **1989**, 139.

When **10** is dissolved in acetonitrile-d_3, a superimposed singlet and doublet centered at 0.56 ppm are observed in the ^{31}P NMR spectrum. The $|^1J(PtP)|$ of this resonance indicates that the both phosphines are still coordinated to the platinum in a cis geometry. This suggests that the acetonitrile-d_3 has displaced the water and ether ligands from **10** to form [*cis*-Pt($CD_3CN)_2${Ph_2P-$(CH_2CH_2O)_4CH_2CH_2PPh_2$}]$(BF_4)_2$ (**11**). The exchange of the free and complexed acetonitrile-d_3 would explain the absence of resonances for coordinated acetonitrile-d_3 in the ^{13}C NMR spectrum of **11**.

The exchange of the free and coordinated acetonitrile-d_3 may also explain the fact that all of the phosphorus-coupled resonances in the ^{13}C NMR spectrum of **11** are doublets. Generally, in cis phosphine complexes, these resonances are apparent quintets (A portions of AXX′ spin systems) because of strong phosphorus–phosphorus coupling (large $^2J(XX')$).[34] This is in spite of the fact that the coupling between phosphorus in one ligand and the carbons in the other ligand ($^4J(AX')$) is zero. Exchange of the acetonitriles and the corresponding exchange of the phosphine groups may decouple the two phosphorus nuclei ($J(XX') = 0$). Then, the ^{13}C nuclei in a ligand would be coupled only to the phosphorus nucleus in that ligand, and the ^{13}C resonances would be doublets.

Summary. Ligands of the type $Ph_2P(CH_2CH_2O)_nCH_2CH_2PPh_2$ (n = 3–5) form mononuclear metallacrown ethers with platinum(II). These metallacrown ethers coordinate alkali metal cations in solution, but this is complicated by solubility changes that occur upon complexation and by loss of the chloride ligands. The X-ray crystal structure of *cis*-$PtCl_2${$Ph_2P(CH_2CH_2O)_4CH_2CH_2PPh_2$} (**5**) suggests that this complex should coordinate most strongly to small cations such as Li^+, while the X-ray crystal structure of *cis*-$PtCl_2${$Ph_2P(CH_2CH_2O)_5CH_2CH_2PPh_2$} (**6**) suggests that this complex should most strongly coordinate to larger cations such as Na^+. These results are consistent with our earlier studies of *cis*-$Mo(CO)_4${$Ph_2P(CH_2CH_2O)_nCH_2CH_2PPh_2$} metallacrown ethers.

The most interesting aspect of this work is the observation that the water molecule in the cationic [Pt{$Ph_2P(CH_2CH_2O)_nCH_2CH_2PPh_2$}$(H_2O)](BF_4)_2$ complex (**10**) is both coordinated to the platinum through the oxygen and hydrogen bonded to two of the ether oxygens of the metallacrown ether ring. This suggests that other ligands such as hydroxide, ammonia, and hydroxycarbonyl, which are capable of both coordination and hydrogen bonding, could be incorporated into similar metallacrown ether complexes. Thus, metallacrown ether complexes may be useful as catalysts for the activation of these small molecules.

Acknowledgment. This work was supported by the donors of the Petroleum Research Fund, administered by the American Chemical Society, and by a generous loan of Pt salts by Johnson Mathey. A.V. thanks the graduate school of the University of Alabama at Birmingham for a Graduate Fellowship. We also greatly appreciate the help of Simon Bott (Chemistry Department of the University of North Texas), Kay Fair (Enraf-Nonius), and Fred Fish (Chemistry Department of the University of Alabama at Birmingham) with the solution and refinement of the X-ray crystal structure of **10**.

Supplementary Material Available: Tables of crystallographic data, thermal parameters, calculated hydrogen positions, other bond lengths and angles, and least-squares planes of the phenyl rings in **5**, **6a**, and **10** (14 pages); tables of observed and calculated structure factors for **5**, **6a**, and **10** (100 pages). Ordering information is given on any current masthead page.

(34) Redfield, D. A.; Nelson, J. H.; Cary, L. W. *Inorg. Nucl. Chem. Lett.* **1974**, *10*, 727.
(35) Johnson, C. F. *ORTEP: A Fortran Thermal-Ellipsoid Program for Crystal Structure Illustrations*; Report ORNL-3974, revised; Oak Ridge National Laboratory: Oak Ridge, TN, 1965.

Contribution from the Centre for Magnetic Resonance, The University of Queensland, Queensland 4072, Australia, Department of Chemistry, Section of Inorganic and Analytical Chemistry, University of Ioannina, 45110 Ioannina, Greece, and NRPCS Demokritos, Institute of Material Science, 15310 Aghia Paraskevi Attikis, Greece

Oxovanadium(IV)–Amide Binding. Synthetic, Structural, and Physical Studies of {*N*-[2-(4-Oxopent-2-en-2-ylamino)phenyl]pyridine-2-carboxamido}oxovanadium(IV) and {*N*-[2-(4-Phenyl-4-oxobut-2-en-2-ylamino)phenyl]pyridine-2-carboxamido}oxovanadium(IV)

Graeme R. Hanson,[1a] Themistoklis A. Kabanos,*[,1b] Anastasios D. Keramidas,[1b] Dimitris Mentzafos,[1c] and Aris Terzis[1c]

Received October 11, 1991

The complexes [VO(pycac)] and [VO(pycbac)] were prepared by the reaction of bis(pentane-2,4-dionato)oxovanadium(IV) with either *N*-[2-(4-oxopent-2-en-2-ylamino)phenyl]pyridine-2-carboxamide (H_2pycac) or *N*-[2-(4-phenyloxobut-2-en-2-ylamino)-phenyl]pyridine-2-carboxamide (H_2pycbac) in a methanolic solution. Crystals of [VO(pycac)] crystallized from nitromethane were monoclinic, space group $P2_1/n$ with a = 7.5938 (1) Å, b = 30.161 (1) Å, c = 13.6982 (2) Å, β = 86.468 (1)°, Z = 8, and R_w = 5.39%. Crystallization of [VO(pycac)] from chlorobenzene yielded triclinic crystals with a space group $P\bar{1}$ and a = 7.8558 (5) Å, b = 12.934 (1) Å, c = 15.675 (1) Å, α = 78.594 (2)°, β = 89.938 (2)°, γ = 88.097 (2)°, Z = 4, and R_w = 6.45%. [VO(pycbac)] crystals were monoclinic, space group $P2_1/c$ with a = 6.5422 (4) Å, b = 14.4786 (8) Å, c = 19.963 (1) Å, β = 93.461 (2)°, Z = 4, and R_w = 3.80%. The geometry about vanadium in each structure approximates a square pyramid with an average V═O bond length of 1.595 Å with the metal ion 0.669 Å above the basal plane. The average V–N(pyridine), V–N(amine), V–N(amide), and V–O bond lengths are 2.100, 2.045, 1.981, and 1.916 Å, respectively. The V–N(amide) and V–O bond lengths constitute rare examples of such short V–N and V–O distances that have been reported for oxovanadium(IV) complexes to date. In addition to the synthesis and crystallographic studies, we report the optical, infrared, magnetic, electron paramagnetic resonance, and electrochemical properties of these complexes. This study represents the first systematic study of oxovanadium containing a vanadium–amide bond.

Introduction

The discovery of vanadium in biomolecules, such as marine algal bromoperoxidase[2,3] nitrogenase from *Azotobacter vinelandii*,[4,5] marine ascidians,[6] and crude oils[7] has produced considerable interest in its biological function.[8] Vanadium may also prove to be a useful therapeutic agent for the treatment of various

* Author to whom correspondence should be addressed.

(1) (a) Centre for Magnetic Resonance, The University of Queensland. (b) Department of Chemistry, Section of Inorganic and Analytical Chemistry, University of Ioannina. (c) NRPCS Demokritos, Institute of Material Science.

